Physics Letters A 384 (2020) 126313

Contents lists available at ScienceDirect

Physics Letters A

www.elsevier.com/locate/pla

Joule-Thomson temperature of a triplon system of dimerized quantum magnets

Abdulla Rakhimov [a,*], Mukhtorali Nishonov [b,c], Bilal Tanatar [a]

[a] Department of Physics, Bilkent University, Bilkent, 06800 Ankara, Turkey
[b] Institute of Nuclear Physics, 100214 Tashkent, Uzbekistan
[c] National University of Uzbekistan, 100174 Tashkent, Uzbekistan

ARTICLE INFO

Article history:
Received 24 November 2019
Received in revised form 31 January 2020
Accepted 4 February 2020
Available online 6 February 2020
Communicated by L. Ghivelder

Keywords:
Triplon
Quantum magnets
BEC
Joule-Thomson coefficient

ABSTRACT

It is well known that, for a system of atomic (molecular) gases both kinds of processes, isentropic as well as isenthalpic are realizable and widely used in refrigeration technique. Particularly, magnetic refrigeration exploits always isentropic process, characterized by Grüneisen parameter $\Gamma_H = (\partial T/\partial H)_S/T$. We propose that, for quantum magnets an isenthalpic (Joule-Thomson) process, characterized by Joule-Thomson coefficient $\kappa_T = (\partial T/\partial H)_W$ may be also available. We considered this effect for a simple paramagnetic and dimerized spin-gapped quantum magnets at low temperatures. We have shown that for both kind of materials refrigeration by using Joule-Thomson effect is more effective than by using ordinary isentropic process, i.e. $\kappa_T > T\Gamma_H$ at low temperatures. For dimerized spin-gapped magnets, where Bose–Einstein condensation of triplon gas may take place, the Joule-Thomson temperature corresponds to the maximal temperature of liquefaction of the triplon system, which is compared with recent experimental observations performed by Dresden group (Wang et al. (2016) [21]). The inversion temperature, where reverse of cooling and heating up regimes takes place, found to be finite for triplons, but infinite for magnons in a simple paramagnetic.

1. Introduction

The properties of dimer spin systems at low temperatures have been intensively investigated in the last two decades. These magnetic systems, e.g., $TlCuCl_3$, $Sr_3Cr_2O_8$, etc. [1] consist of weakly coupled dimers with strong antiferromagnetic interaction between spins within a dimer. The ground state in such components is singlet and it is separated from the first exited triplet state by a gap at zero magnetic field at zero temperature that may be interpreted as a liquid behavior characterized by a finite correlation length [2]. When an external magnetic field H is applied, the gap can be closed due to the Zeeman effect, resulting in the generation of a macroscopic number of triplet excitations (triplons) and the transition to a magnetically ordered phase takes place at $H = H_c$. This transition has been observed by studying the magnetization M of e.g., $TlCuCl_3$ nearly 20 years ago [3]. Further, it was shown that it may be effectively described in terms of Bose–Einstein condensation (BEC) of quasi-particles of triplons [4,5], which mathematically can be introduced by a generalized Schwinger representation in the bond-operator formalism [6,7]. In a constant external magnetic field and zero temperature the number of triplons is conserved in the thermodynamic limit and controlled by an effective chemical potential μ defined as [7–9]

$$\mu = g_f \mu_B (H - H_c), \tag{1}$$

where g_f is electron Lande factor and μ_B is the Bohr magneton.

A triplon does not carry mass or electric charge, but a magnetic moment. Thus, it can be easily understood that the total density of triplons, ρ defines the uniform magnetization M, while the number of condensed triplons N_0 defines the staggered magnetization M_{stag}, namely [3]

$$M = g_f \mu_B N, \tag{2}$$

$$M_{stag} = g_f \mu_B \sqrt{\frac{N_0}{2}}. \tag{3}$$

Here it should be noted that, in the thermodynamic limit, BEC is accompanied by spontaneous breaking of global gauge symmetry, which is a necessary and sufficient condition [7]. But in real materials, e.g. in $TlCuCl_3$, this symmetry can be explicitly broken due to anisotropy. As a result, instead of a phase transition one has to deal

* Corresponding author.
E-mail addresses: rakhimovabd@yandex.ru (A. Rakhimov), nishonov@inp.uz (M. Nishonov), tanatar@fen.bilkent.edu.tr (B. Tanatar).

https://doi.org/10.1016/j.physleta.2020.126313
0375-9601/

with a crossover where the staggered magnetization is renormalized [10–12]. In the present work, for simplicity we shall neglect such effects and exploit Eqs. (2) and (3).

At zero temperature $T = 0$, BEC is considered as a quantum phase transition (QPT), which occurs upon tuning an external parameter. For ordinary gases this parameter is, naturally, the gas pressure, P, while for the system of triplons it may be identified as the external magnetic field. Pursuing the analogy between these two systems one may arrive at many interesting universal conclusions. For instance, recently, Garst et al. [13] have considered the Grüneisen parameter Γ and the magnetocaloric effect (MCE) near a pressure (for gases) and magnetic field controlled QPT, respectively. Using scaling analysis they have shown that the Grüneisen parameter defined as

$$\Gamma = \begin{cases} \frac{1}{C_P V}\left(\frac{\partial V}{\partial T}\right)_P = \frac{1}{VT}\left(\frac{dT}{dP}\right)_S \equiv \Gamma_P, \text{ gases} \\ -\frac{1}{C_H}\left(\frac{\partial M}{\partial T}\right)_H = \frac{1}{T}\left(\frac{dT}{dH}\right)_S \equiv \Gamma_H, \text{ magnets} \end{cases} \tag{4}$$

(where V is volume, C_P is heat capacity at constant pressure and C_H is heat capacity at constant H) changes its sign near generic quantum critical points. Recently, we have shown that [14] for spin gapped dimerized magnets this characteristic point coincides with the critical temperature of triplon condensation T_c. The position of such a point indicates the accumulation of entropy in the phase diagram. From the definition in Eq. (4) it is understood that Γ_P and Γ_H correspond to pressure-caloric and magneto-caloric isentropic effects at constant entropy, $S = \text{const.}$, for gases and for paramagnets, respectively. Here, it should be underlined that Γ_H is one of the key parameters of magnetic refrigeration at cryogenic temperatures and a highly topical area of research has been triggered by the observation of a giant MCE around room temperature [15,16].

The investigation of analogy between ordinary gases and the system of magnons has been further advanced by Bovo et al. [17]. Studying frustrated ferromagnets, they have found that analogous to gases, magnets have at least two kinds of critical temperature, namely Joule T_J and Joule-Thomson T_{JT} temperatures. By definition T_J corresponds to the temperature for which the system is quasi-ideal and the internal energy E is independent of the extensive parameters such as volume (cf. Table I of Ref. [17]), $(\partial E/\partial V)_T = 0$, or magnetization $(\partial E/\partial M)_T = 0$. As to the T_{JT}, it is related to the well known Joule-Thomson isenthalpic process which is characterized by the following coefficient

$$\kappa_{JT} = \begin{cases} \left(\frac{\partial T}{\partial P}\right)_W = \frac{1}{C_P}\left[T\left(\frac{\partial V}{\partial T}\right)_P - V\right], \\ \text{gases} \\ \left(\frac{\partial T}{\partial H}\right)_W = \frac{1}{C_H}\left[M - T\left(\frac{\partial M}{\partial T}\right)_H\right]. \\ \text{paramagnets} \end{cases} \tag{5}$$

The sign of κ_{JT} indicates whether the system heats up ($\kappa_{JT} > 0$) or cools ($\kappa_{JT} < 0$) during the process when the intensive parameter, P or H is increased. By definition the Joule-Thomson temperature, referred in literature also as an inversion temperature, is the temperature when κ_{JT} changes its sign i.e., $\kappa_{JT}(T = T_{JT}) = 0$. Note that for a classical ideal gas $\kappa_{JT} = 0$ at any temperature whereas ideal quantum gases have non-zero κ_{JT} at low temperature [18]. Such a quantum isenthalpic process has been recently observed in a saturated homogeneous Bose gas [19].

In practice T_{JT} shows the starting of the regime below which a gas may be liquefied by the Linde-Hampson isenthalpic process. For example for helium $T_{JT} = 34$ K, which means that one has to cool helium down to 34 K to obtain liquid helium using the Joule-Thomson effect. In Refs. [20,21] it has been argued that a 3D spin-dimerized quantum magnet exhibits a triplon liquid phase between H_{c_1} and H_{c_2} (saturation field). As to the superfluid phase it is embedded in a dome-like phase diagram of triplon liquid extending up to T_c^{max}, maximum temperature of the magnetically ordered regime [21–23], as it is illustrated in Fig. 4 of Ref. [21]. Particularly, $T_c^{max} \leq 9$ K both for $Sr_3Cr_2O_8$ and $TlCuCl_3$.

As discussed by Wang et al. [21] the ground-state of such a system is a quantum disordered paramagnet with a spin gapped elementary excitation, triplon. When Zeeman energy compensates the intra-dimer interaction, a QPT from quantum disordered (QD) phase to a spin aligned state can be induced. The paramagnetic and ferromagnetic states are separated by a canted-XY antiferromagnetic phase, which can be viewed as a triplon superfluid. The superfluid fraction survives up to $T_c^{max} \approx 8$ K and the triplon exhibit liquid-like behavior up to some temperature denoted by T^* ($T^* \sim 18$ K), as it was confirmed by analyzing the sound velocity measurements. Now, coming back to the analogy with ordinary atomic systems, we may argue that in spin-dimerized magnets T_c corresponds to the critical temperature of BEC, while T_{JT} being the maximal temperature of liquefaction corresponds to T^* of Ref. [21], i.e., to the temperature below which triplons may be considered to be in the liquid phase. In other words, we assume that similarly to ordinary gases, T_{JT} is the temperature above which the triplon gas can not be "liquefied". Therefore, the main purpose of the present work is to study possible Joule-Thomson effect on dimerized spin-gapped quantum magnets and to estimate its inversion temperature T_{JT}. As to the temperature T_J, which has rather academic interest, a reader may refer to our previous work [24].

The rest of the paper is organized as follows. In Sect. 2 we present general analytical expressions of magnetic thermodynamics. Then in Sect. 3 we consider the case of quantum magnets and derive equations for main thermodynamic quantities. Having performed numerical study which we present in Sect. 4 we discuss our predictions concerning the inversion temperature T_{JT} and efficiency of isenthalpic MCE. The main conclusions are drawn in Sect. 5. The details of some calculations are moved to the Appendices A and B.

2. Basic relations of magnetic thermodynamics

Generally speaking, the total Hamiltonian (or energy) of a magnetic substance is usually assumed to consist of several contributions: the crystalline lattice ($\hat{H}_L$), the conducting electrons ($\hat{H}_e$), the magnetic moments ($\hat{H}_m$) and the atomic nucleus ($\hat{H}_n$). So are the thermodynamic potentials, e.g. the grand potential Ω and the entropy, S.

For the sake of simplicity, we assume that Ω_L and Ω_e do not depend on the applied magnetic field but only on the temperature, and hence the total changes induced by the magnetic field variation are attributed to the changes of only the magnetic part. Below we concentrate only on the magnetic part, denoting it $\Omega_M = \Omega$. In the next section we derive Ω explicitly for spin gapped magnets while here we present some general relations, assuming that Ω is known.

We have the following relations for main thermodynamic potentials [25]

$$\begin{aligned} &F = \Omega + \mu N, E = F + TS, \quad \Phi = W - TS = \mu N \\ &W = E + PV - HM = \mu N + TS, \end{aligned} \tag{6}$$

where E, F, W and Φ are internal energy, Gibbs free energy, enthalpy and Helmholtz potential, respectively. The total differentials are [26,27]

$$\begin{aligned} d\Omega &= -SdT - PdV - Nd\mu - MdH, \\ dF &= -SdT - PdV + \mu dN + HdM, \\ dE &= TdS - PdV + \mu dN + HdM, \end{aligned} \tag{7}$$

$$d\Phi = -SdT + VdP + \mu dN - MdH,$$
$$dW = TdS + VdP + \mu dN - MdH.$$

Now passing to the discussion of the Joule-Thomson temperature T_{JT} we lay out some equivalent relations for the magnetic Grüneisen parameter which characterizes the isentropic ($\Delta S = 0$) process

$$\Gamma_H = \frac{1}{T}\left(\frac{\partial T}{\partial H}\right)_S = -\frac{1}{C_H}\left(\frac{\partial M}{\partial T}\right)_H = -\frac{1}{C_H}\left(\frac{\partial S}{\partial H}\right)_T \tag{8}$$

where C_H is defined as $C_H = T\left(\frac{\partial S}{\partial T}\right)_H = \left(\frac{\partial W}{\partial T}\right)_H$. These equations can be derived easily using Eqs. (6) and (7) and well-known Maxwell relations.

An isenthalpic process ($W = \text{const.}$) being the main part of Joule-Thomson effect is characterized by the Joule-Thomson coefficient $\kappa_{JT} \equiv (\partial T/\partial H)_W$ (similar to $\kappa_{JT} \equiv (\partial T/\partial P)_W$ for atomic gases). As it was shown in Appendix A, κ_{JT} can be represented as

$$\kappa_{JT} = \frac{1}{C_H}\left[M - T\left(\frac{\partial M}{\partial T}\right)_H\right] = \frac{M}{C_H} + T\Gamma_H\,. \tag{9}$$

Finally, the inversion temperature T_{JT} is the solution of $\kappa_{JT}(T = T_{JT}) = 0$, which leads to

$$\frac{d(\chi/T)}{dT}\Big|_{T=T_{JT}} = 0, \tag{10}$$

where we defined the susceptibility $\chi(T, H)$ as[1]

$$\chi \equiv \frac{M}{H}. \tag{11}$$

Using Eqs. (9)–(11) we can see that at the inversion temperature T_{JT} the quantity χ/T has a local extremum, i.e., $d(\chi/T)/dT$ changes its sign. Equations (6)-(10) are general for any paramagnetic material. In the next section we derive thermodynamic quantities specifically for spin gapped dimerized quantum magnets.

3. Magnetic thermodynamics of spin gapped antiferromagnets

Microscopically, properties of any magnetic material may be described by a Heisenberg-like Hamiltonian [27]. However, Giamarchi and Tsvelik [28] have shown that the Hamiltonians of quantum antiferromagnets and BECs are directly related to each other by a mapping transformation. In fact, using the bond operator formalism [6] the Hamiltonian of the triplon gas may be simplified to the following semi-phenomenological Hamiltonian [1]

$$H = \int d\vec{r}\left\{\Psi^\dagger\left[\hat{K} - \mu\right]\Psi + \frac{U}{2}(\Psi^\dagger\Psi)^2\right\} \tag{12}$$

where Ψ is the bosonic field, μ is the chemical potential given in Eq. (1), and U is a coupling constant of triplon-triplon contact interaction, which is usually considered as a fitting parameter. The kinetic energy operator, $\hat{K}$ gives rise to the bare disperison ε_k as defined, for example, in the bond operator representation [29,30]. As to the integration in coordinate space, it should be taken within the crystal unit cell, though some authors take the integration within a sphere of infinite radius [4,31].

[1] The Eq. (11) should be considered just as a notation, not a linear approximation, which holds for a weak magnetic field.

Applying the concept of BEC to the system of triplons, we have recently obtained [14] an explicit expression for Ω in the Hartree-Fock-Bogoliubov approximation, which gives the following equations for physical quantities under consideration:

- Critical temperature of BEC T_c is given by the equation

$$\sum_k \frac{1}{e^{\varepsilon_k/T_c} - 1} = \frac{\mu}{2U} \tag{13}$$

Here and what follows the summation over $\vec{k}$,

$$(1/V)\sum_k = \int d^3\vec{k}/(2\pi)^3$$

implies the integration over the first Brilloin zone: $\mathbf{B} = \{-\pi \le k_\alpha \le \pi\}$ with $\alpha = x, y, z$. As to ε_k – bare dispersion of triplons, strictly speaking, one should use a realistic dispersion, taking into account possible anisotropies, [5,30]. However, for qualitative analysis a simple ansatz [2,4]

$$\varepsilon_k = J_0(3 - \cos ak_x - \cos ak_y - \cos ak_z) \tag{14}$$

is also good, where $m = 1/J_0$ is an effective mass of triplon. Note that, the ordinary spherical symmetric bare dispersion, $\varepsilon_k = \vec{k}^2/2m$, which is used for atomic gases, leads to the well-known result

$$T_c^0 = \frac{2\pi}{m}\left(\frac{\rho_c}{\zeta(3/2)}\right)^{2/3} \tag{15}$$

where ρ_c is critical density which can be experimentally measured and $\zeta(x)$ is the Riemann zeta function.

- Entropy, specific heat and Grüneisen parameter are given by the following expressions

$$S = -\left(\frac{\partial\Omega}{\partial T}\right)_H = -\sum_k \ln\left[1 - e^{-\beta\mathcal{E}_k}\right] + \beta\sum_k \frac{\mathcal{E}_k}{e^{\beta\mathcal{E}_k} - 1} \tag{16}$$

$$C_H = T\left(\frac{\partial S}{\partial T}\right)_H = \beta^2\sum_k \frac{\mathcal{E}_k(\mathcal{E}_k - T\mathcal{E}'_{k,T})e^{\beta\mathcal{E}_k}}{\left(e^{\beta\mathcal{E}_k} - 1\right)^2} \tag{17}$$

$$\Gamma_H = -\frac{g_f\mu_B}{C_H}\left(\frac{\partial S}{\partial\mu}\right)_T = \frac{g_f\beta^2\mu_B}{C_H}\sum_k \frac{\mathcal{E}_k\mathcal{E}'_{k,\mu}e^{\beta\mathcal{E}_k}}{\left(e^{\beta\mathcal{E}_k} - 1\right)^2} \tag{18}$$

where $\beta = 1/T$ and Ω, $\mathcal{E}'_{k,T} = (\partial\mathcal{E}_k/\partial T)_H$, $\mathcal{E}'_{k,\mu} = (\partial\mathcal{E}_k/\partial\mu)_T$ are given explicitly in Appendix B. In the above equations $\mathcal{E}_k$ corresponds to the quasiparticle dispersion

$$\mathcal{E}_k = \begin{cases} \omega_k = \varepsilon_k - \mu_{eff} & \text{for } T \ge T_c \\ E_k = \sqrt{\varepsilon_k}\sqrt{\varepsilon_k + 2\Delta} & \text{for } T < T_c \end{cases} \tag{19}$$

with $\mu_{eff} = \mu - 2U\rho$.

- The total number of triplons and the number of condensed ones are given as

$$N = \begin{cases} \sum_k \frac{1}{e^{\beta\omega_k}-1} & \text{for } T > T_c \\ \frac{(\Delta+\mu)}{2U} & \text{for } T \le T_c \end{cases} \tag{20}$$

$$N_0 = \begin{cases} 0 & \text{for } T > T_c \\ N - \sum_k \left[\frac{W_k(\varepsilon_k+\Delta)}{E_k} - \frac{1}{2}\right] & \text{for } T \le T_c \end{cases} \tag{21}$$

where Δ is the anomalous self-energy Σ_{an} in the BEC phase. It can be evaluated as the physical solution ($\Delta \ge 0$) of following algebraic equation [31]

$$\Delta = \mu - 2\sum_k \left[\frac{W(\beta E_k)(\varepsilon_k + 2\Delta)}{E_k} - \frac{1}{2}\right] \tag{22}$$

where $W(x) = \coth(x/2)/2 = 1/2 + 1/(\exp(x)-1)$. It is seen from Eq. (19) that in the BEC phase the dispersion is gapless and defines the sound velocity c as $c = \sqrt{\Delta/m}$ due to the low momentum expansion $E_k = ck + O(k^2)$.

It should be noted that in this section and below we adopt the units $k_B = 1$ for the Boltzmann constant, $\hbar = 1$ for the Planck constant, and V=1 for the unit cell volume.

4. Results and discussions

To perform numerical calculations we adopt commonly used set of realistic parameters g_f, H_c, U and J_0, which have been fitted to experimental data for $Sr_3Cr_2O_8$ and $TlCuCl_3$ [20,32,33], as presented in Table 1.

As it was mentioned in the Introduction section, we assume that besides the well known adiabatic (isentropic) MCE, there can be another version of MCE, which exploits an isenthalpic process. In the present section we first compare them with each other and then pass to discuss the inversion temperature.

For simplicity we start with a paramagnetic material whose magnetization is given as [34]

$$M = g_f \mu_B \tanh(x) \tag{23}$$

where $x = g_f \mu_B H/T$. Now,

$$\left(\frac{\partial T}{\partial H}\right)_S = T\,\Gamma_H = \frac{g_f \mu_B x}{C_H \cosh^2(x)}, \tag{24}$$

for isentropic and

$$\left(\frac{\partial T}{\partial H}\right)_W = \kappa_{JT} = \frac{g_f \mu_B}{C_H}\left[\tanh(x) + \frac{x}{\cosh^2(x)}\right] \tag{25}$$

for isenthalpic processes, respectively. Their ratio may simply be represented as

$$r_{SW} \equiv \frac{\left(\frac{\partial T}{\partial H}\right)_S}{\left(\frac{\partial T}{\partial H}\right)_W} = \frac{x}{\tanh(x)\,\cosh^2(x) + x}. \tag{26}$$

The function $r_{SW}(x)$ is plotted in Fig. 1. It is seen that for reasonable values of the $x = 0 \div 5$, this quantity is less than unity, i.e., $r_{SW} < 1$, which means that isentropic process is less effective than isenthalpic one for a paramagnet. Here the influence of other parameters of MCE are neglected. From Eq. (24) one may note that $\Gamma_H \ge 0$ and $\Gamma_H(x=0) = 0$. So is the Joule-Thomson coefficient given by Eq. (25) and hence, T_{JT} (paramagnetic) $\to \infty$.

Now, we pass to dimerized quantum magnets. In Fig. 2 (a) and Fig. 2 (b) we present $(\partial T/\partial H)_S = T\Gamma_H$ vs temperature for $Sr_3\ Cr_2O_8$ and $TlCuCl_3$. As it is expected Γ_H changes its sign at $T = T_c$ which means that in the isentropic process the regime of heating ($T < T_c, \Gamma_H > 0$) changes by the regime of cooling ($T > T_c, \Gamma_H < 0$) at the critical temperature with increasing magnetic field.[2]

Table 1
Material parameters used in our numerical calculations. From the experimental input parameters g_f and H_c we derived J_0 and coupling constant U by fitting the experimental phase boundary $T_c(H)$ to Eqs. (1) and (13) (see Ref. [14] for the details).

	g_f	H_c (T)	J_0 (K)	U (K)
$Sr_3Cr_2O_8$	1.95	30.4	15.86	51.2
$TlCuCl_3$	2.06	5.1	50	315

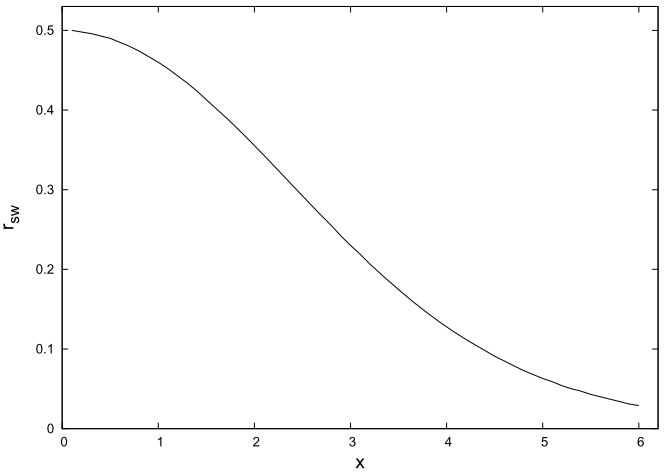

Fig. 1. The ratio $r_{SW} = (dT/dH)_S/(dT/dH)_W$ vs the parameter $x = g_f \mu_B H/T$ for a simple paramagnet. As it is seen $r_{SW} < 1$ for moderate values of x.

On the other hand, the changing of the temperature as the magnetic field varies in the isenthalpic process $(\partial T/\partial H)_W = \kappa_{JT}$ is presented in Fig. 3(a,b) for $Sr_3Cr_2O_8$ and $TlCuCl_3$, respectively. Comparing the absolute values of $(\partial T/\partial H)_S$ and $(\partial T/\partial H)_W$ for the same values of T and H (e.g., Fig. 2(a) with Fig. 3(a)) one may note that especially, at low temperatures

$$\left|(\partial T/\partial H)_S\right|_{T\le 3K} < \left|(\partial T/\partial H)_W\right|_{T\le 3K} \tag{27}$$

i.e., isenthalpic preocess is more effective than isentropic one. Moreover, as it is seen from Figs. 3, κ_{JT} diverges at low temperature, which is caused by the divergence of Grüneisen parameter [13,14] and $1/C_H$ term in Eq. (9).

Now we discuss the inversion temperature T_{JT} of these compounds. As it is seen from Figs. 3(a,b) magnetic Joule-Thomson coefficient κ_{JT} crosses the abscissa at a moderate value of the temperature. Therefore, in contrast to a simple paramagnet, the inversion temperature for dimerized magnets is finite. To study this point in more detail we shall look for a possible extremum of the function $\chi(T,H)/T$, in accordance with the Eq. (10).

In Fig. 4(a,b) we present $d(\chi/T)/dT$ vs temperature for $Sr_3Cr_2O_8$ ($H = 33\,T$) and $TlCuCl_3$, ($H = 6\,T$), respectively. It is seen that $d(\chi/T)/dT$ changes its sign at temperatures higher than critical one, $T_{JT} > T_c$. This can be easily understood from Eq. (9) and Fig. 2: for $T < T_c$ the parameter Γ_H is positive, and hence $\kappa_{JT}(T)$ may not reach zero.

We address the question of information that can be extracted from experiments, say, from the extremum of the function χ/T, which is related to $M(T,H)$. Unfortunately, there is no experimental data on $M(T)$ available for $Sr_3Cr_2\ O_8$, but there is a plenty of

[2] In the present work we are dealing with only magnetic contribution, so the terms "heating" or "cooling" mean the changing of the temperature only due to the spins.

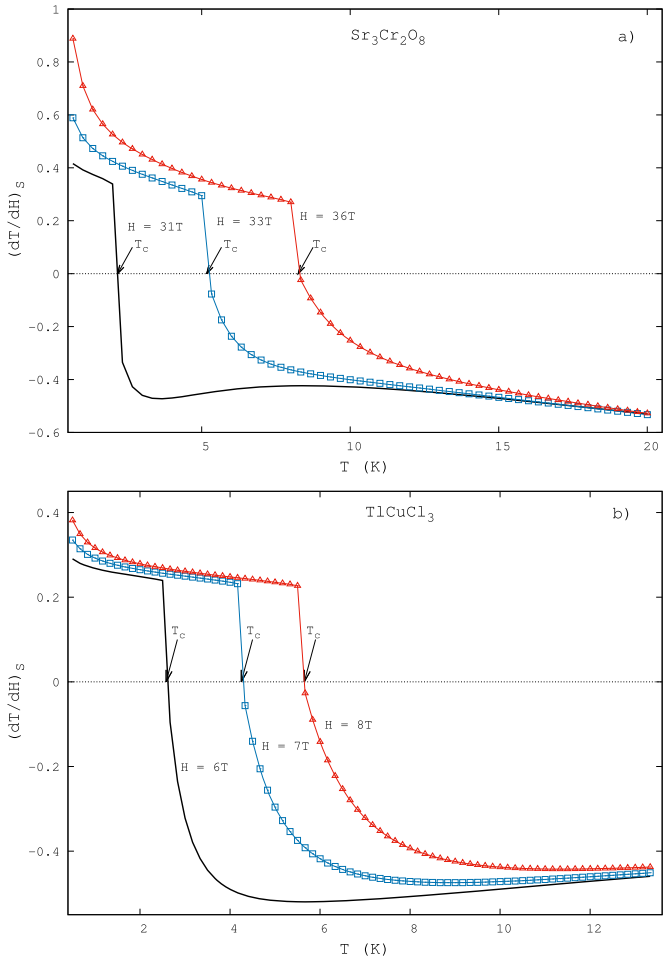

Fig. 2. The Gruneisen parameter multiplied by temperature, $T\Gamma_H = (dT/dH)_S$ in units of KT^{-1} for various magnetic fields and for compounds (a) $Sr_3Cr_2O_8$ and (b) $TlCuCl_3$.

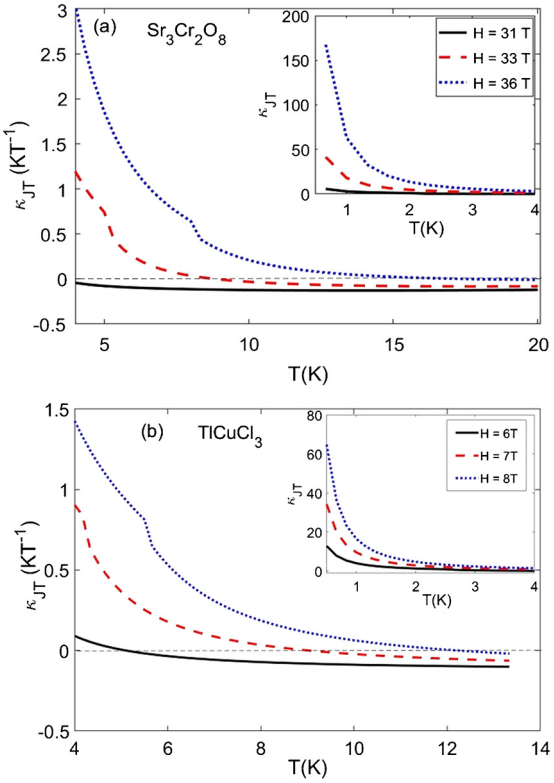

Fig. 3. The temperature dependence of the Joule-Thomson coefficient for $Sr_3Cr_2O_8$ (a) and $TlCuCl_3$ (b) The point where κ_{JT} crosses abscissa corresponds to inversion temperature for each magnetic field. Inset: κ_{JT} at low temperatures.

data on $M(T)$ for $TlCuCl_3$ [4,32]. Thus, we have explored the existing data on $M(T, H)$ for this material, e.g., given in Ref. [32] and using Eq. (11), constructed the dependence of $d(\chi/T)/dT$ on temperature. From Fig. 4b we see that the experimental value of T_{JT} for $TlCuCl_3$ at $H = 6T$ is $T_{JT}^{exp}(H = 6T) \approx 3.9K$. This fact confirms the existence of a finite inversion temperature for the compound $TlCuCl_3$, which has no frustration. As to our theoretical prediction, it is seen that, the solid line in Fig. 4(b) (inset) crosses the abscissa at a larger temperature, approximately at $T_{JT}^{HFB}(H = 6T) \approx 5K$. It appears that our estimate is in good qualitative agreement with the experiment. As it is seen from Figs. 4, at low temperatures, $d(\chi/T)/dT < 0$ and divergent. This can be easily understood from its equivalent expression as $d(\chi/T)/dT = -(\Gamma_H C_H + MT^{-1})/HT$.

Similarly to the inversion temperature of atomic gases, which depends on pressure, the inversion temperature of a magnetic Joule-Thomson process depends on the external magnetic field, which is presented in Figs. 5(a,b). As it is seen, for both materials this temperature is larger than the critical temperature of BEC, and the dependence of the dimensionless ratio T_{JT}/T_c on the magnetic field is rather small.

As it is mentioned in the Introduction the Dresden group [21] have performed measurements for $Sr_3Cr_2O_8$ in the temperature region $T > T_c$. Particularly, they have observed that in the region of temperatures $8\,\mathrm{K} \leq T < 18\,\mathrm{K}$ the sound velocity, and hence bulk modulus have an anomaly which disappears at $T = T^* \sim 18$ K [22].

Following their interpretation this fact may provide experimental evidence of the existence of a field induced triplon liquid in the 3D spin-dimerized quantum antiferromagnet $Sr_3Cr_2O_8$ and the maximal temperature of liquefaction, T^*. Thus, proceeding with the analogy of atomic and triplon gases one may come to the conclusion that the inversion temperature T_{JT} under consideration is nothing but the temperature T^* found in their work. Actually, as it is seen from Fig. 5(a) the predicted Joule-Thomson temperature is $T_{JT}^{max} = 17.5$ K (at $H = 36$ T), which in good agreement with the experimental $T^* \sim 18$ K.

5. Conclusion

We have utilized the BEC analogy to study magnetic thermodynamics of dimerized $s = 1/2$ quantum magnets. For this purpose we derived explicit expressions for the main thermodynamic quantities within the Hartree-Fock-Bogoliubov approximation. These equations, as well as experimental data, have shown that when the external magnetic field exceeds a critical one, $H > H_c$ the system of triplons has at least two finite characteristic temperatures: T_{JT} and T_c. The former presents a signature of the liquid state in a temperature region $T \leq T_{JT}$, while the latter which corresponds to the critical temperature of BEC, $T_c < T_{JT}$ shows also the point when in the triplon liquid a finite superfluid component arises. In this sense, the present work gives an additional argument in order to affirm that the field induced triplons in 3D spin-dimerized antiferromegnets could be in the liquid state in the range of temperatures $T \leq T_{JT}$, where the Joule-Thomson temperature T_{JT} is finite and of the order of the critical temperature of BEC, $T_{JT} \sim 1.8T_c$.

Comparing commonly used isentropic (adiabatic) MCE with a proposed isenthalpic process we have shown that the latter is more powerful both for simple paramagnetics as well as dimerized magnets. We hope that such a process can be realized in pressure and field induced magnetic experiments.

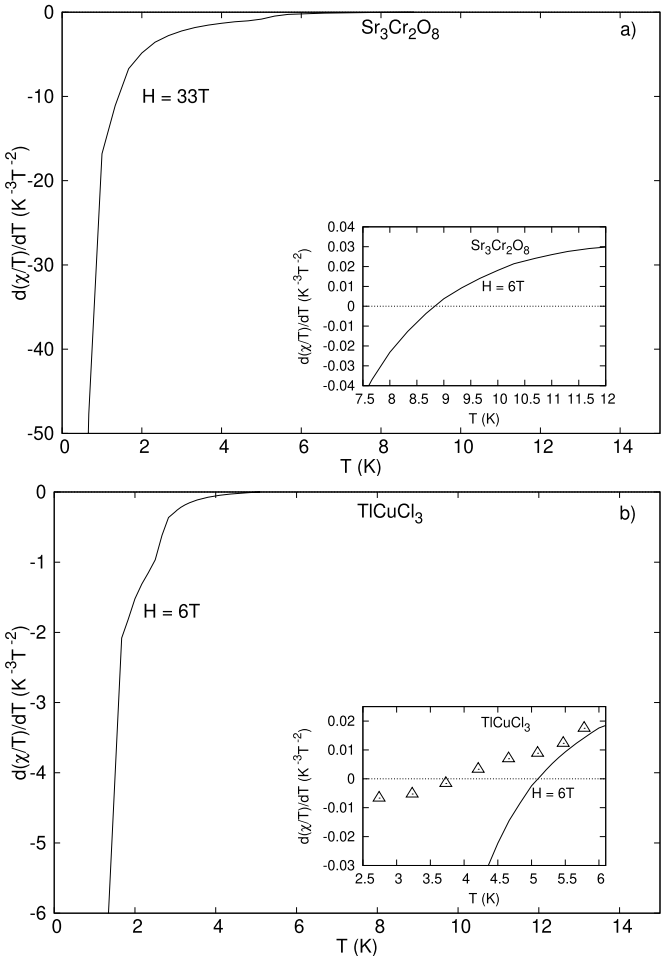

Fig. 4. The quantity $d(\chi/T)/dT$ vs temperature for (a) $Sr_3Cr_2O_8$ and (b) $TlCuCl_3$. The point where it changes its sign corresponds to the inversion temperature. The insets show the same quantity around $T \sim T_{JT}$. The triangles correspond to $d(\chi/T)/dT$ extracted from the experimental data on $M(T)$ for $TlCuCl_3$ from Ref. [32].

Unfortunately, the present simple approach cannot describe saturation effects, since they are not included in the effective Hamiltonian (12) properly. Besides, for simplicity anisotropic effects, which are essential [10,11] for $TlCuCl_3$ due to Dzyaloshinsky-Moriya (DM) or exchange anisotropy (EA) interactions are neglected. Nevertheless, our predictions on the inversion temperature are in a good qualitative agreement with the existing experimental observations. As to the isenthalpic magneto-caloric effect, proposed in present work, more experimental studies on the thermodynamic properties of field or pressure induced phase transitions should be performed. The situation may be the similar with high temperature superconductors, whose critical temperature changes under high pressure [35]. Here it is worth to underline that the thermodynamics of pressure and field induced phase transitions in spin-dimerized magnets have not been fully explored [36].

Acknowledgements

We are indebted to Andreas Schilling and Adam Aczel for discussions. We thank Zhe Wang, S. Zherlitsyn for a useful communication. This work is partially supported by the Turkish Scientific and Technological Research Council-Bilim Insanı Destekleme Daire Başkanlığı (TUBITAK-BIDEB) Program 2221 and Turkish Academy of Sciences (TUBA) Grant No. AD-20. A. R. and M. N. acknowledge the funding from Academy of Sciences of the Republic of Uzbekistan through Grant No. FPFI F.2-18.

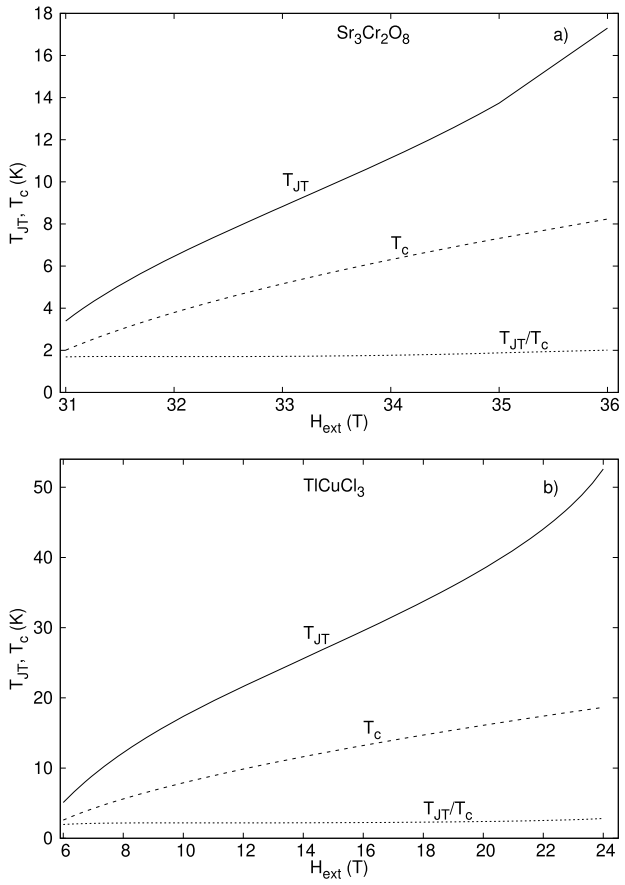

Fig. 5. The magnetic field dependence of the inversion temperature T_{JT} (solid), critical temperature T_c (dashed) and the ratio T_{JT}/T_C (dotted) for $Sr_3Cr_2O_8$ (a) and $TlCuCl_3$ (b).

Appendix A

Here we derive explicit expression for κ_{JT} given by Eq. (9). Indeed, starting from

$$\kappa_{JT} = \left(\frac{\partial T}{\partial H}\right)_W \tag{A.1}$$

$$= \frac{\frac{\partial(T,W)}{\partial(H,T)}}{\frac{\partial(H,W)}{\partial(H,T)}} = \frac{\left(\frac{\partial T}{\partial H}\right)_T \left(\frac{\partial W}{\partial T}\right)_H - \left(\frac{\partial T}{\partial T}\right)_H \left(\frac{\partial W}{\partial H}\right)_T}{\left(\frac{\partial H}{\partial H}\right)_T \left(\frac{\partial W}{\partial T}\right)_H - \left(\frac{\partial H}{\partial T}\right)_H \left(\frac{\partial W}{\partial H}\right)_T}$$

$$= -\frac{1}{C_H}\left(\frac{\partial W}{\partial H}\right)_T, \tag{A.2}$$

and using Eq. (7) it is easy to show that

$$\left(\frac{\partial W}{\partial H}\right)_T = T\left(\frac{\partial S}{\partial H}\right)_T - M \tag{A.3}$$

and

$$\left(\frac{\partial S}{\partial H}\right)_T = -\frac{\partial}{\partial H}\left(\frac{\partial \Phi}{\partial T}\right)_H = -\frac{\partial}{\partial T}\left(\frac{\partial \Phi}{\partial H}\right)_T$$

$$= \left(\frac{\partial M}{\partial T}\right)_H. \tag{A.4}$$

Inserting (A.3) and (A.4) into (A.2) finally gives κ_{JT} in (9).

Appendix B

Here we present explicit expressions for the free energy, obtained in our earlier work [14] using a variational perturbative

theory [37,38]. In the normal $T > T_c$ and ordered $T \leq T_c$ phases it is given by

$$\Omega(T > T_c) = -UN^2 + T\sum_k \ln(1 - e^{-\beta\omega_k}) \tag{B.1}$$

and

$$\Omega(T \leq T_c) = \frac{1}{2}\sum_k (E_k - \varepsilon_k) + T\sum_k \ln(1 - e^{-\beta E_k}) + U\rho_1(\rho_1 - 2N) - \frac{\Delta^2}{2U} \tag{B.2}$$

where

$$\Delta = \mu + 2U(\sigma - \rho_1), \tag{B.3}$$

$$\sigma = -\Delta\sum_k \frac{W_k}{E_k}, \tag{B.4}$$

$$\rho_1 = \sum_k \left[\frac{W_k(\varepsilon_k + \Delta)}{E_k} - \frac{1}{2}\right], \tag{B.5}$$

with $W_k = \frac{1}{2}\coth\left(\frac{\beta E_k}{2}\right)$, $E_k = \sqrt{\varepsilon_k(\varepsilon_k + 2\Delta)}$.

Now we bring explicit expressions for $\mathcal{E}'_{k,T} = (\partial\mathcal{E}_k/\partial T)_H$ and $\mathcal{E}'_{k,\mu} = (\partial\mathcal{E}_k/\partial\mu)_T$ which were used to calculate C_H and Γ_H in the Section 3.

In the normal phase when $\mathcal{E}_k = \omega_k = \varepsilon_k - \mu + 2U\rho$, the density of particles is given by

$$\rho = \sum_k f_B(\omega_k) \tag{B.6}$$

where $f_B(x) = 1/(e^{\beta x} - 1)$. Clearly,

$$\frac{d\omega_k}{dT} = 2U\frac{d\rho}{dT} \tag{B.7}$$

which does not depend on momentum k. Differentiating both sides of the equation (B.6) with respect to T and solving by dp/dT, we find

$$\frac{d\rho}{dT} = \frac{\beta S_1}{(2S_2 - 1)}, \tag{B.8}$$

$$S_1 = -\beta\sum_k \omega_k f_B^2(\omega_k)e^{\omega_k\beta},$$

$$S_2 = -U\beta\sum_k f_B^2(\omega_k)e^{\omega_k\beta}. \tag{B.9}$$

Taking the derivative with respect to μ gives

$$\frac{d\omega_k}{d\mu} = 2U\frac{d\rho}{d\mu} - 1,$$

$$\frac{d\rho}{d\mu} = \frac{S_2}{U(2S_2 - 1)}. \tag{B.10}$$

In the condensed phase, $T \leq T_c$, $\mathcal{E}_k = E_k = \sqrt{\varepsilon_k(\varepsilon_k + 2\Delta)}$, and hence we have

$$\frac{dE_k}{dT} = \frac{\varepsilon_k}{E_k}\Delta'_T,$$

$$\frac{dE_k}{d\mu} = \frac{\varepsilon_k}{E_k}\Delta'_\mu. \tag{B.11}$$

To find, e.g., Δ'_T we can differentiate both sides of the equation (B.3) with respect to T and solve it for Δ'_T.

The results are

$$\Delta'_T = \frac{d\Delta}{dT} = \frac{gS_4}{2T(2S_5 + 1)},$$

$$\Delta'_\mu = \frac{d\Delta}{d\mu} = \frac{1}{2S_5 + 1},$$

$$S_4 = \sum_k W'_k(\varepsilon_k + 2\Delta), \tag{B.12}$$

$$S_5 = U\sum_k \frac{4W_k + E_k W'_k}{4E_k},$$

where

$$W'_k = \beta(1 - 4W_k^2). \tag{B.13}$$

References

[1] V. Zapf, M. Jaime, C.D. Batista, Bose–Einstein condensation in quantum magnets, Rev. Mod. Phys. 86 (2014) 563.

[2] T. Giamarchi, C. Rüegg, O. Tchernyshyov, Bose–Einstein condensation in magnetic insulators, Nat. Phys. 4 (2008) 198.

[3] H. Tanaka, A. Oosawa, T. Kato, H. Uekusa, Y. Ohashi, K. Kakurai, A. Hoser, Field-induced three-dimensional magnetic ordering in the spin-gap system $TlCuCl_3$, J. Phys. Soc. Jpn. 70 (2001) 939.

[4] F. Yamada, T. Ono, H. Tanaka, G. Misguich, M. Oshikawa, T. Sakakibara, Magnetic-field induced Bose–Einstein condensation of magnons and critical behavior in interacting spin dimer system $TlCuCl_3$, J. Phys. Soc. Jpn. 77 (2008) 013701.

[5] C. Rüegg, N. Cavadini, A. Furrer, H.-U. Gudel, K. Kramer, H. Mutka, A. Wildes, K. Habicht, P. Vorderwisch, Bose–Einstein condensation of the triplet states in the magnetic insulator $TlCuCl_3$, Nature (London) 423 (2003) 62.

[6] S. Sachdev, R.N. Bhatt, Bond-operator representation of quantum spins: mean-field theory of frustrated quantum Heisenberg antiferromagnets, Phys. Rev. B 41 (1990) 41.

[7] V.I. Yukalov, Difference in Bose–Einstein condensation of conserved and unconserved particles, Laser Phys. 22 (2012) 1145.

[8] T. Radu, H. Wilhelm, V. Yushankhai, D. Kovrizhin, R. Coldea, Z. Tylczynski, T. Lühmann, F. Steglich, Bose–Einstein condensation of magnons in Cs_2CuCl_4, Phys. Rev. Lett. 95 (2005) 127202.

[9] D.L. Mills, Comment on Bose–Einstein condensation of magnons in Cs_2CuCl_4, Phys. Rev. Lett. 98 (2007) 039701.

[10] J. Sirker, A. Weisse, O.P. Sushkov, Consequences of spin-orbit coupling for the Bose–Einstein condensation of magnons, Europhys. Lett. 68 (2004) 275.

[11] A. Khudoyberdiev, A. Rakhimov, A. Schilling, Bose–Einstein condensation of triplons with a weakly broken U(1) symmetry, New J. Phys. 19 (2017) 113002.

[12] A.K. Kolezhuk, V.N. Glazkov, H. Tanaka, A. Oosawa, Dynamics of an anisotropic spin dimer system in a strong magnetic field, Phys. Rev. B 70 (2004) 020403(R).

[13] M. Garst, A. Rosch, Sign change of the Grüneisen parameter and magnetocaloric effect near quantum critical points, Phys. Rev. B 72 (2005) 205129.

[14] A. Rakhimov, A. Gazizulina, Z. Narzikulov, A. Schilling, E.Y. Sherman, Magnetocaloric effect and Grüneisen parameter of quantum magnets with a spin gap, Phys. Rev. B 98 (2018) 144416.

[15] M. Lang, B. Wolf, A. Honecker, Y. Tsui, D. Jaiswal-Nagar, U. Tutsch, G. Hofmann, A. Prokofiev, P.T. Cong, N. Krüger, F. Ritter, W. Assmus, Magnetic cooling through quantum criticality, J. Phys. Conf. Ser. 400 (2012) 032043.

[16] B. Wolf, A. Honecker, W. Hofstetter, U. Tutsch, M. Lang, Cooling through quantum criticality and many-body effects in condensed matter and cold gases, Int. J. Mod. Phys. B 28 (2014) 1430017.

[17] L. Bovo, M. Twengström, O.A. Petrenko, T. Fennell, M.J.P. Gingras, S.T. Bramwell, P. Henelius, Special temperatures in frustrated ferromagnets, Nat. Commun. 9 (2018) 1999.

[18] H. Saygın, A. Şişman, Joule-Thomson coefficients of quantum ideal-gases, Appl. Energy 70 (2001) 49.

[19] T. Schmidutz, I. Gotlibovych, A.L. Gaunt, R.P. Smith, N. Navon, Z. Hadzibabic, Quantum Joule-Thomson effect in a saturated homogeneous Bose gas, Phys. Rev. Lett. 112 (2014) 040403.

[20] A.A. Aczel, Y. Kohama, C. Marcenat, F. Weickert, M. Jaime, O.E. Ayala-Valenzuela, R.D. McDonald, S.D. Selesnic, H.A. Dabkowska, G.M. Luke, Field-induced Bose–Einstein condensation of triplons up to 8 K in $Sr_3Cr_2O_8$, Phys. Rev. Lett. 103 (2009) 207203.

[21] Z. Wang, D.L. Quintero-Castro, S. Zherlitsyn, S. Yasin, Y. Skourski, A.T.M.N. Islam, B. Lake, J. Deisenhofer, A. Loidl, Field-induced magnonic liquid in the 3D spin-dimerized antiferromagnet $Sr_3Cr_2O_8$, Phys. Rev. Lett. 116 (2016) 147201.

[22] Z. Wang, D.L. Quintero-Castro, S. Zherlitsyn, S. Yasin, Y. Skourski, A.T.M.N. Islam, B. Lake, J. Deisenhofer, A. Loidl, Erratum: Field-induced magnonic liquid in the 3D spin-dimerized antiferromagnet $Sr_3Cr_2O_8$, Phys. Rev. Lett. 117 (2016) 189901.

[23] J. Brambleby, P.A. Goddard, J. Singleton, M. Jaime, T. Lancaster, L. Huang, J. Wosnitza, C.V. Topping, K.E. Carreiro, H.E. Tran, Z.E. Manson, J.L. Manson, Adiabatic physics of an exchange-coupled spin-dimer system: magnetocaloric effect, zero-point fluctuations, and possible two-dimensional universal behavior, Phys. Rev. B 95 (2017) 024404.
[24] A. Rakhimov, B. Tanatar, L. Rani, M. Nishonov, Characteristic temperatures of a triplon system of dimerized quantum magnets, arXiv:1903.08438, 2019.
[25] L.D. Landau, E.M. Lifshitz, Statistical Physics, Part 1, 3rd ed., Elsevier Butterworth-Heinemann, 1980.
[26] V.I. Yukalov, Theory of cold atoms: basics of quantum statistics, Laser Phys. 23 (2013) 062001.
[27] W. Nolting, A. Ramakanth, Quantum Theory of Magnetism, Springer, 2009.
[28] T. Giamarchi, A.M. Tsvelik, Coupled ladders in a magnetic field, Phys. Rev. B 59 (1999) 11398.
[29] M. Matsumoto, B. Normand, T.M. Rice, M. Sigrist, Field- and pressure-induced magnetic quantum phase transitions in $TlCuCl_3$, Phys. Rev. B 69 (2004) 054423.
[30] G. Misguich, M.J. Oshikawa, Bose–Einstein condensation of magnons in $TlCuCl_3$: phase diagram and specific heat from a self-consistent Hartree-Fock calculation with a realistic dispersion relation, J. Phys. Soc. Jpn. 73 (2004) 3429.
[31] A. Rakhimov, S. Mardonov, E.Y. Sherman, Macroscopic properties of triplon Bose–Einstein condensates, Ann. Phys. 326 (2011) 2499.
[32] R. Dell'Amore, A. Schilling, K. Krämer, Fraction of Bose–Einstein condensed triplons in $TlCuCl_3$ from magnetization data, Phys. Rev. B 78 (2008) 224403.
[33] Y. Kohama, C. Marcenat, T. Klein, M. Jaime, AC measurement of heat capacity and magnetocaloric effect for pulsed magnetic fields, Rev. Sci. Instrum. 81 (2010) 104902.
[34] C. Kittel, Introduction to Solid State Physics, 8th ed., John Wiley and Sons, New York, 1986.
[35] L.P. Gor'kov, V.Z. Kresin, Colloquium: High pressure and road to room temperature superconductivity, Rev. Mod. Phys. 90 (2018) 011001.
[36] P. Merchant, B. Normand, K. Krämer, M. Boehm, D.F. McMorrow, C. Rüegg, Quantum and classical criticality in a dimerized quantum antiferromagnet, Nat. Phys. 10 (2014) 373.
[37] H. Kleinert, Z. Narzikulov, A. Rakhimov, Quantum phase transitions in optical lattices beyond the Bogoliubov approximation, Phys. Rev. A 85 (2012) 063602.
[38] A. Rakhimov, C.K. Kim, S.-H. Kim, J.H. Yee, Stability of the homogeneous Bose–Einstein condensate at large gas parameter, Phys. Rev. A 77 (2008) 033626.